International Journal of Solids and Structures 50 (2013) 4133–4144

Contents lists available at ScienceDirect

International Journal of Solids and Structures

journal homepage: www.elsevier.com/locate/ijsolstr

Influence of partial constrained layer damping on the bending wave propagation in an impacted viscoelastic sandwich

Boubaker Khalfi *, Annie Ross

CREPEC, Department of Mechanical Engineering, École Polytechnique de Montréal, P.O. Box 6079, Station Centre-ville, Montréal H3C 3A7, Canada

ARTICLE INFO

Article history:
Received 26 February 2013
Received in revised form 20 July 2013
Available online 1 August 2013

Keywords:
Sandwich
Plate
Transient response
Damping
Impact
Wave propagation

ABSTRACT

This paper presents a parametric model to study the transient bending wave propagation in a viscoelastic sandwich plate due to impact loading. The effect of partial constrained layer damping (PCLD) geometry on wave propagation is investigated by comparing with propagation in single layer elastic plate. Several boundary conditions are also considered, and their effect on wave propagation is highlighted.

The equation of motion is obtained from Lagrange's equations. For the single layer plate, the governing equation is solved in time domain using Newman and Wilson method. For the plate with PCLD, the frequency dependant viscoelastic behavior of the core is represented by Prony series; the equation of motion is converted into frequency domain using Fourier transform the displacement is obtained in the frequency domain and is converted into time domain with the Inverse Fast Fourier Transform.

The model was validated in our previous paper (Khalfi and Ross (2013)) with experimental results, additional validation is carried in this paper with literature, and good agreement is recorded. The results show that the plate covered with PCLD remains a dispersive medium. The shape of the wave is mainly related to the sandwich stiffness while the viscoelastic layer contributes in reducing the amplitude and speed of propagation. The particularity of this transient model lies in its ability to follow the shape of the bending wave at all times to observe formation, propagation and disappearance. With this model, the influence of any structural input parameters on the bending wave can be studied. The findings presented will also serve as a research base for more advanced horizons.

1. Introduction

The use of plates and shells in the industry becomes increasingly important. However, transient phenomena are associated with the assembly process, causing vibrations and noise. In particular, the sound produced by riveting or other processes requiring impacts may exceed the limits allowed by safety standards, causing growing concern of workplace health and safety organizations.

Among solutions used to reduce the sound generated by the impacted plates, we find the passive damping or Partial Constrained Layer Damping (PCLD). In this technique, the base plate (BP), which is the plate to be damped, is partially covered with a surface treatment that consists of a viscoelastic material layer (VEM) and a constraining plate (CP). The VEM is sandwiched between the base plate and constraining plate. In most cases, the constraining layer is made of the same material as the base plate or another material with similar stiffness. During the structure vibrations, the strain of the constraining layer could be controlled by a special set-up. In addition to the base plate and the viscoelestic layer, we find: Amplifier, Piezo-electric constraining layer. Baz (1997), in this case we deal with the active damping. The active damping is used in the applications where the weight is critical. Many works was performed by Baz et al., such as Baz and Ro (1996), in this paper it was presented the main step of the technique for a rectangular plate, while in Ray et al. (2001) it was studied the case of cylindrical shell. In Baz and Ro (1995, 1997, 1998) they study the optimization techniques. In Baz and Ro (1999) they study the control of sound radiation from a plate into an acoustic cavity with active damping. Recently Horodinca (2013) study the optimal design problem for a cantilever beam with active damping. The beam was subjected to static and dynamic loading on its free side. A non linear transient analysis of adaptative beam was studied by Deu et al. (2008), they focus their study on developing a beam element type that allows a large displacement and rotation, they used finite elements method and they solved the equation of motion with incremental iterative method.

In this paper we focus the study on the passive damping. Different aspects of research can be developed on this subject, such as the dynamic response of the sandwich due to impact, or the influence of the geometric properties of the PCLD on the transient response and acoustic wave propagation in the sandwich. In this paper, we focus the analysis on the propagation of bending waves

* Corresponding author. Tel.: +1 5143404711.
E-mail addresses: boubaker.mohamed@polymtl.ca (B. Khalfi), annie.ross@polymtl.ca (A. Ross).

0020-7683/$ - see front matter Crown Copyright © 2013 Published by Elsevier Ltd. All rights reserved.
http://dx.doi.org/10.1016/j.ijsolstr.2013.07.023

in the plate and the influence of the PCLD geometry on the wave propagation. Sun and Luo (2011) studied the wave propagation and transient response of an "*infinite functionally graded plate*" (viscoelastic layer sandwiched between two dissimilar homogeneous plates). They used the high-order shear deformation theory and included the effect of the rotational inertia in the governing equation. They used a simple power law distribution along the thickness to vary the material properties of the sandwich, and defined the volume fraction of each face plate as $((2Z + h)/2\,h)^N$, where h is thickness of the layer, Z is height with respect to neutral line and N is volume fraction index. They showed that for a given wave number, the plate frequency, and the group velocity of the wave decrease as the layers volume fraction index increases.

Liu and Bhattacharya (2009) studied the propagation of elastic waves in a sandwich structure with two thin face sheets and a thick core. By considering Hamilton's principle and transfer matrix approach, they presented a complete description of the dispersion; in addition, they deduced a relationship giving all the natural frequencies of the sandwich. Akbarov et al. (2011) used 3D theory to show that initial strain limits the propagation of extensional waves and Lamb waves in the sandwich plate. Shorter (2004) developed a spectral finite element method based on high degree polynomial basis, for analyzing wave propagation and damping in linear viscoelastic laminates. He determined the wave type (progressive or evanescent) and estimated the loss factor from strain energy distribution. Edward and Kerwin (1959) studied the influence viscoelastic core on flexural vibration of a plate. They showed that the damping factor depends on the thickness, wavelength, and elastic modulus of the plates. Haikuo et al. (2011) used wave propagation for damage detection in thick beam based on 3D spectral element method. They concluded that when the thickness of the beam is close to the wavelength of elastic bending wave, a local wave mode exists simultaneously with quasi-symmetric and anti-symmetric wave modes. Kudela et al. (2007) studied the wave propagation in a composite plate. They used spectral element method to solve the problem and to show that the velocity of bending waves is correlated with fiber orientation and volume fraction. Roy (2005) observed bending wave propagation in a plate partially covered with Vac Damp (a vacuum applied PCLD) from experiments and using an analytical model. The results showed that wave speed and amplitude are affected by PCLD. Effect of mechanical discontinuity at the borders of the PCLD is also highlighted. Oulmane (2007) studied wave propagation in a rectangular plate by carrying out finite element analyses. They plot the transverse displacement in sections of the plate, and they used this tool to highlight the effect of discontinuity created by PCLD on wave propagation. In addition, they concluded that the damping of wave depends on PCLD characteristics, as well as the position.

Even though many studies were performed, a lot of issues still need to be examined. These issues, which are the purpose of this paper, are related to boundary conditions and the characteristics of the PCLD (thickness of layers and position). For all these parameters, we will not only relate the response of the plate to the input parameter, but also we will analyze the evolution of the initial bending wave during the transient regime.

In this paper, the analytical model used is briefly described, since the detailed model was presented in our previous paper.-Khalfi and Ross (2013). Two analyses are performed. The first study is carried out on a rectangular plate without PCLD, in which we consider three boundary conditions for all edges:

- simply supported;
- clamped;
- free.

The second analysis is carried out on a PCLD treated plate; the geometric parameters of the PCLD are considered to identify their influences on wave propagation:

- thickness of layers;
- position of PCLD.

2. Model

In this section, only the main steps of the model are described, in order to point out at elements that are necessary for our discussion. The sandwich studied is shown in Fig. 1. In this figure, a simply supported plate (BP) is padded with PCLD composed of VEM layer and constraining plate (CP). The different dimensions used in the model are also indicated.

In Fig. 1, subscripts b, c, and v refer to the base plate, constraining plate, and VEM, respectively. The transverse displacement is denoted by w, while the displacements in the x and y directions are denoted by u and v respectively. Thicknesses are denoted by h_i $(i = b,c,v)$. We assume that the three layers undergo the same transversal displacement; this assumption requires that the three layers are perfectly bonded, and that compression in the VEM is negligible. In addition, shear deflection and rotation inertia in the base plate and constraining plate are neglected. Finally, the VEM carries only transverse shear and no normal stress, while the shear modulus (Eq. (1)) is assumed complex and frequency dependent. The Prony series in the frequency domain is used to reflect its behavior (Granger and Ross, 2009):

$$G(\omega) = G_0\left[1 - \sum_{n=1}^{N} g_n + \sum_{n=1}^{N} \frac{j\omega g_n \tau_n}{1 + j\omega\tau_n}\right] \tag{1}$$

where τn are called relaxation times, g_n are Prony constants, $G_0 = G(t = 0)$, ω is the frequency, N is the number of Prony constants and $j = \sqrt{-1}$.

The displacement is expressed using the assumed modes technique. In this method, the displacement is expressed as the product of two functions satisfying the boundary conditions; one function

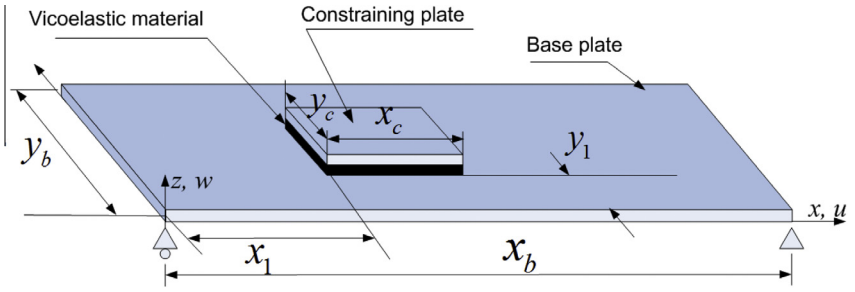

Fig. 1. Simply supported sandwich plate.

Table 1
Mechanical properties and number of modes.

Young modulus (GPa)	Shear modulus (GPa)	Poisson ratio	Density (kg/m^3)		Damping ratio of the VEM	Number of modes		
Eb, Ec	G_v	vb, vc	ρb, ρc	ρv	ξ	nw	nb	nc
69.8	0.869	0.33	2700	999	0.5	200	30	30

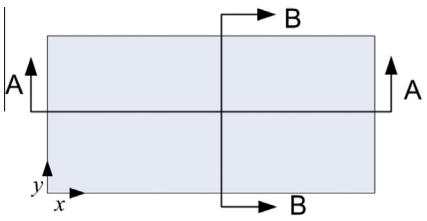

Fig. 2. Sandwich sections.

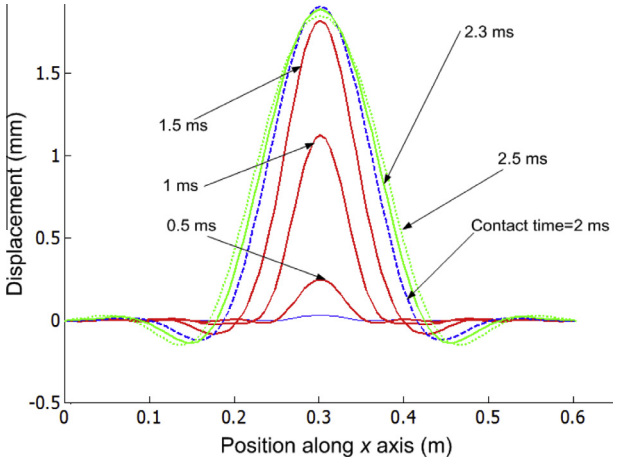

Fig. 3. Simply supported plate, transversal displacement in section A–A.

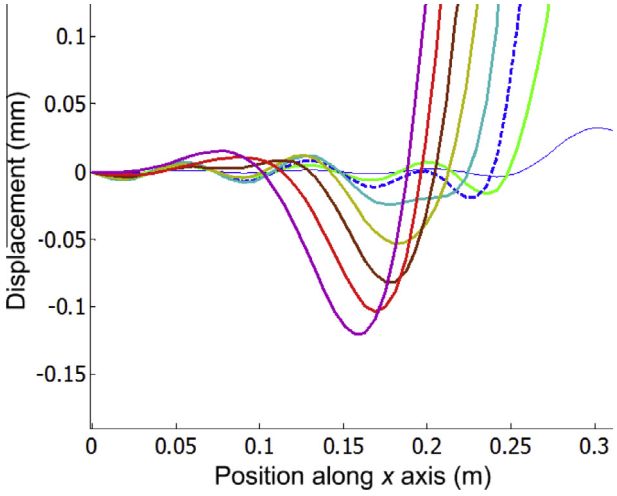

Fig. 4. Evolution of wave fronts.

is time dependent, and the other is dependent on space. This expression is written as:

$$X(x,y,t) = \sum_{i=1}^{n} \Gamma_i(x,y)\xi_i(t) \tag{2}$$

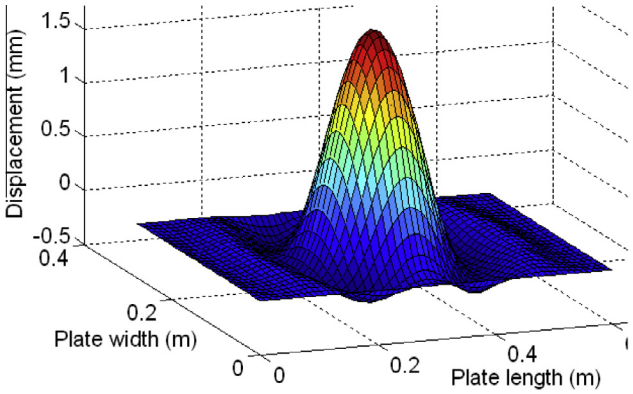

Fig. 5. 3D Plate deformation at contact time.

Where X is the displacement, Γ_i are the admissible functions (given in Appendix A), ξ_i are the new generalized coordinates, n takes into account n_b and n_c, the number of modes used for the longitudinal displacements of the BP and CP, respectively, and n_w, the number of modes for the flexural motion of the sandwich. The equation of motion is derived from the Lagrange's equations, where the total strain energy U and kinetic energy K of the sandwich are used to calculate the Lagrangian:

$$L = K - U \tag{3}$$

$$\frac{\partial}{\partial t}\left(\frac{\partial L}{\partial \dot{\xi}_i}\right) - \frac{\partial L}{\partial \xi_i} = Q_i \tag{4}$$

where Q_i the generalized forces:

$$Q_i = -\partial S/\partial \dot{\xi}_i + \partial P/\partial \xi_i \tag{5}$$

are obtained by differentiation of Rayleigh's dissipation function S and virtual work P done by external forces. Replacing displacement by its expression (Eq. (2)), in system (4) and developing the calculation, we obtain the following system:

$$[M]\ddot{X} + [K]X = Q \tag{6}$$

where M is the mass matrix and K is the complex stiffness matrix. The impact force (Eq. (7)) is modeled by Heitkämper's relation (Blais, 2009):

$$F(t) = F_0 \left[\begin{array}{l} \left(\frac{1.1}{1+\Lambda+2\Lambda^2}\right) \sin(0.97T)^{1.5} \exp\left(-(0.4T)^4\right) \\ +\left(\frac{1+2/\Lambda}{1+\Lambda}\right)\left(\frac{T}{T+1/\Lambda}\right)^{1.5} \exp\left(\frac{-T}{\Lambda}\right) \end{array} \right] \tag{7}$$

where $T = \pi t/T_0$, T_0 is the contact duration, F_0 is the force amplitude, and Λ is an impact parameter that depends on the geometrical and mechanical properties of the two bodies.

To conduct a transient analysis of the system subjected to impact excitation, the solution of Eq. (6) can be obtained by two methods. The first one, which is performed in time domain, is based on iterative techniques(Cho et al., 2000). This method has the advantage of avoiding time aliasing, which appears in spectral analysis of low damping systems. In this paper, we use the Newmark and Wilson method (Cho et al., 2000) for the unpadded (single layer) plate. For the plate with PCLD, the shear modulus is

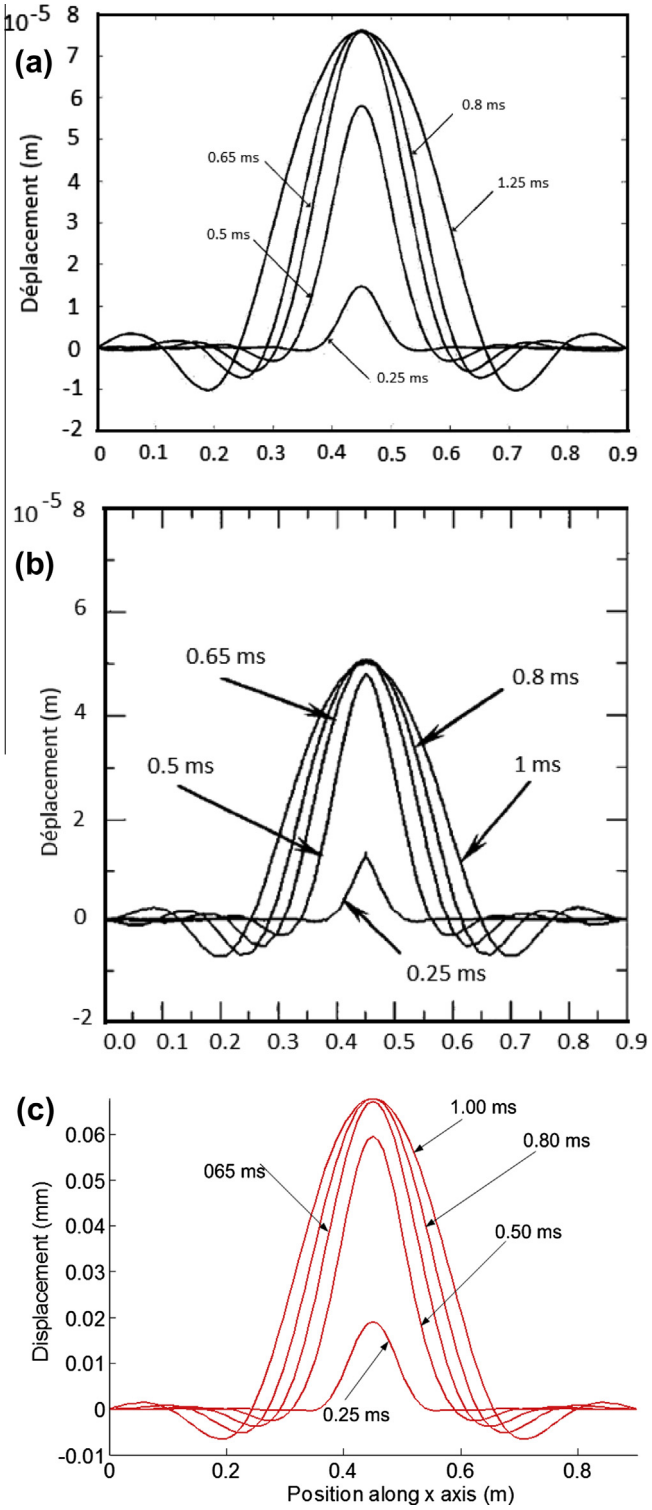

Fig. 6. Transversal displacement section at $y = yb/2$, (a) from Roy (2005), (b) from Oulmane (2007) and (c) present model.

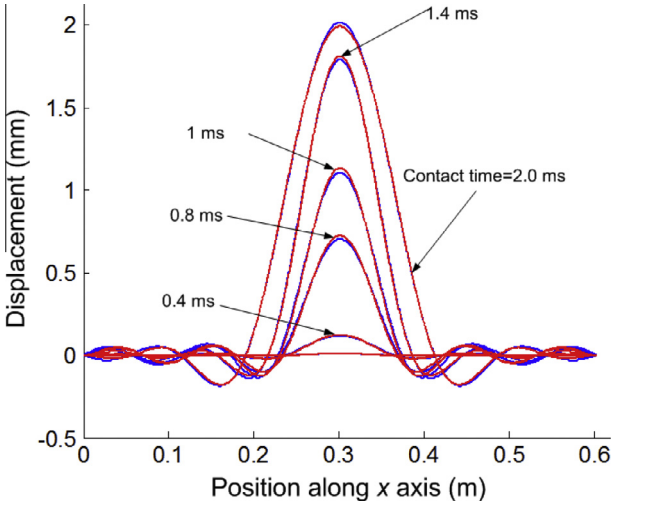

Fig. 7. Transversal displacement in section A–A: (comparison CC and SS plate during contact time).

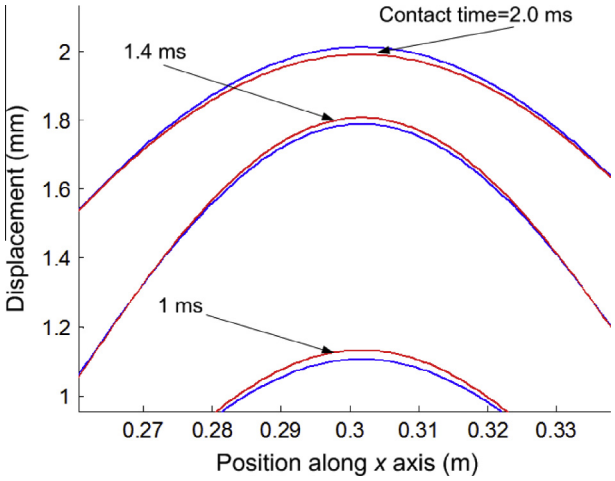

Fig. 8. Close-up view of Fig. 7.

poorly represented in the time domain; it is therefore more convenient to work in the frequency domain, as established by Barkanov et al. (2000). For this reason, a second method is used in frequency domain. Eq. (6) and the impact force are converted to the Fourier domain via Fast Fourier Transform (FFT). Once the solution obtained, it is converted back to the time domain via Inverse Fast Fourier Transform IFFT.

3. Analysis and discussion

Two analyses are performed in this section. First we study the influence of boundary conditions on the flexural wave propagation for the untreated plate. In the second analysis, we study the influence of PCLD geometry on the wave propagation for a simply supported plate with PCLD. The base plate is made of aluminum with the following dimensions: 601 mm × 283 mm × 0.793 mm. The

Table 2
Mechanical properties of the plate used by Roy (2005) and Oulmane (2007).

Young modulus	Dimensions	Poisson ratio	Density	τ	F_{max}	Λ
71.00 GPa	0.9 m × 0.6 m × 4.8 mm	0.33	2714 Kg/m^3	0.00065 s	148 N	1.0

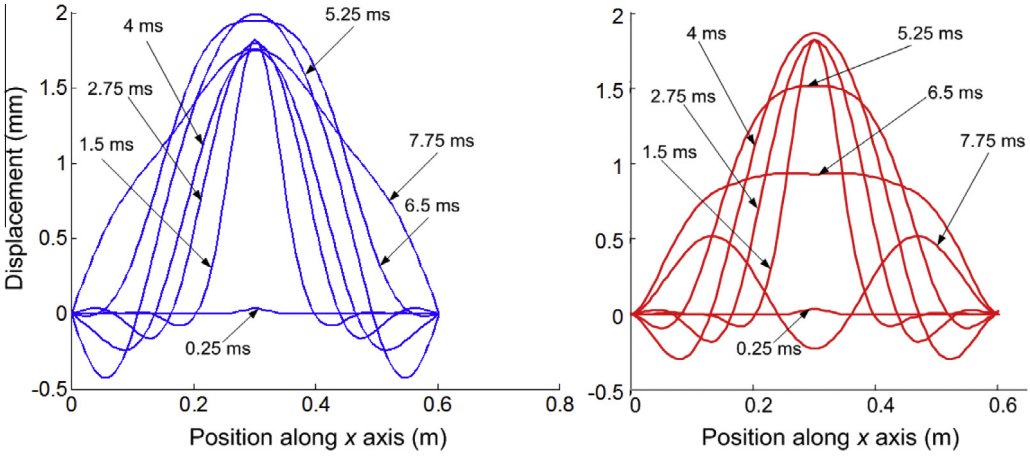

Fig. 9. Transversal displacement in section A–A after end-of-contact: (SSSS (left) and CCCC (right)).

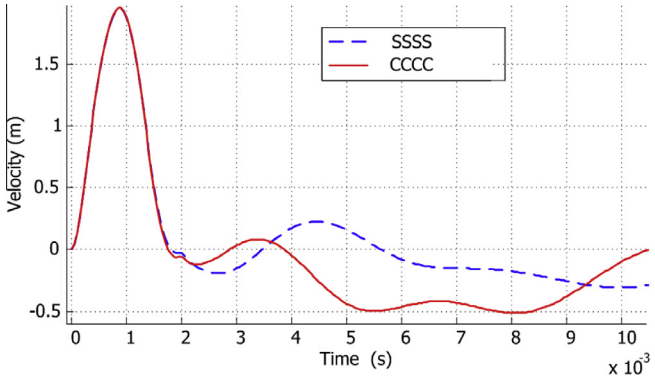

Fig. 10. Transverse velocities: (clamped plate (CCCC) and simply supported plate (SSSS)).

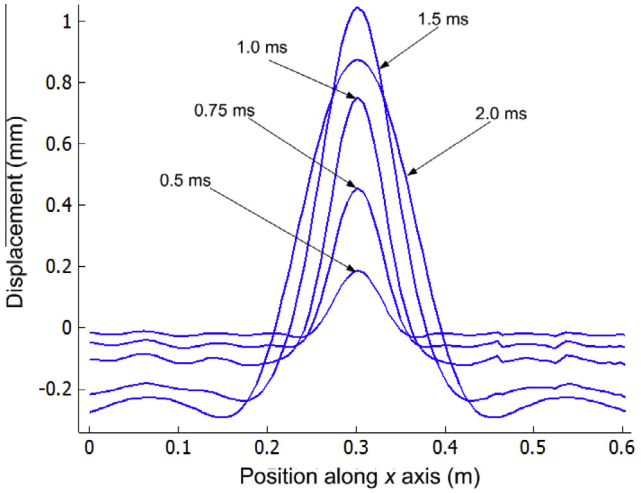

Fig. 11. Transversal displacement in section A–A: free edge plate (FFFF).

mechanical properties used for the sandwich are shown in Table 1. The characteristics of the force, calculated by Eq. (7), are: F_0 = 102.6 N, τ = 0.002 s, Λ = 1.0. These values are used in all simulations, unless otherwise indicated.

3.1. Plate without PCLD

In this section, the governing equation is solved in the time domain using Newman and Wilson's method. Impacts are simulated and the general characteristics of bending wave propagation in the simply supported plate are first described. Then, the influence of boundary conditions and impact location are discussed. All displacement results are given either for section A-A or for section B–B, both shown in Fig. 2.

3.1.1. Wave propagation in the plate

Fig. 3 displays the transverse displacement in section A–A of the plate (see Fig. 2) for an impact taking place at the center of the plate ($x = x_b/2; y = y_b/2$). As expected due to the symmetry of the plate, the response of the plate, which is made of a main crest surrounded by side crests, is symmetrical. The highest crest takes place at the point of impact. This crest increases with time until the end-of-contact time (2 ms); it then starts to decrease. In Fig. 4, side crests are shown with a closer view. The curves describe the evolution of wave fronts located on both sides of the main crest. From the dashed line curve, we see how the secondary crests move towards the edges, while the main crest widens. These results are in good agreement with the work done by Roy, 2005. Fig. 5 illustrates perfectly the deformation in the entire plate at the end-of-contact time, and is in good agreement with Oulmane (2007).

Fig. 6 compares transverse displacements in section A–A obtained by the present model (Fig. 6(c), numerical values are provided in Table 3 for purpose of validation), and the ones obtained by Roy (2005) (Fig. 6(a)), and Oulmane (2007) (Fig. 6(b)). The plate studied is simply supported, made from aluminium, with the following characteristics (see Eq. 7 for parameters description):

In Table 2, F_{max}, which represents the maximum value reached by the force, is different from the parameters F_0 in Eq. (7). Oulmane obtained his results by finite element analysis, while Roy used a rudimentary analytical model. These graphs show that the general motion obtained is very similar in all three analyses. The maximum amplitude varies between 0.05 mm (Oulmane, 2007) and 0.075 mm (Roy, 2005); the value for the present study (0.065 mm) is in between.

The conclusion to be drawn from this section is that the present model reflects well the behavior of the plate.

3.1.2. Influence of boundary conditions

In this section, simply supported (SSSS), clamped (CCCC) and free (FFFF) boundary conditions are compared. These conditions are the same on all edges of the plate. The plate dimensions are 601 mm × 283 mm × 0.793 mm. Fig. 7 shows a comparison between the transverse displacements in section A–A for cases SSSS and CCCC, and Fig. 8 displays a close-up of the main crest near the end-of-contact time. It is seen from these figures that during

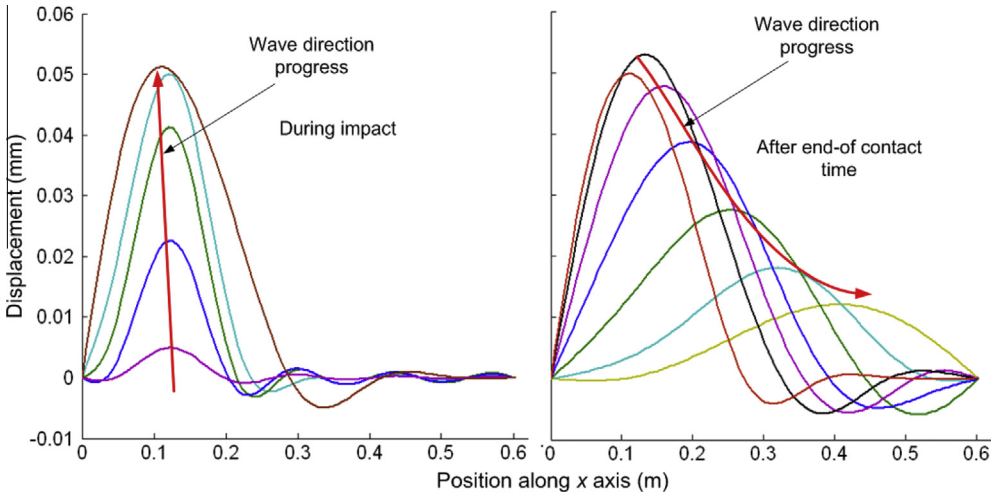

Fig. 12. Transversal displacement in section A–A for SSSS condition (impact at:$x = x_b/5$, $y = y_b/2$: during impact (left) and after end-of-contact time (right)).

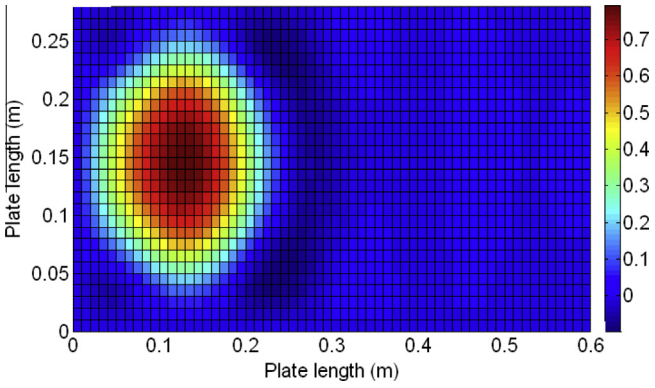

Fig. 13. 2D Plate deformation at end-of-contact time (impact at $x = x_b/5$; $y = y_b/2$).

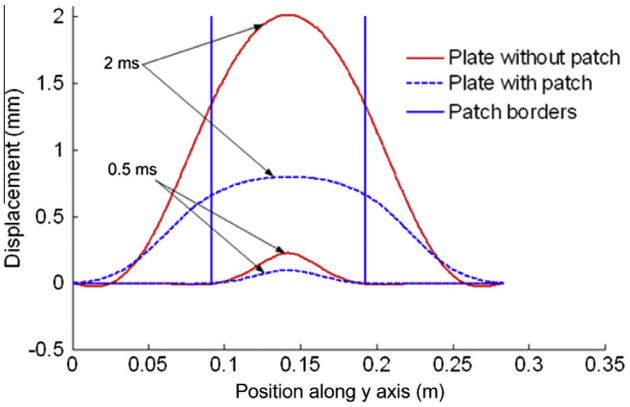

Fig. 15. Comparison between plate with and without PCLD (transverse displacement in section B–B, $h_c = 0.79$ mm, $h_v = 0.127$ mm).

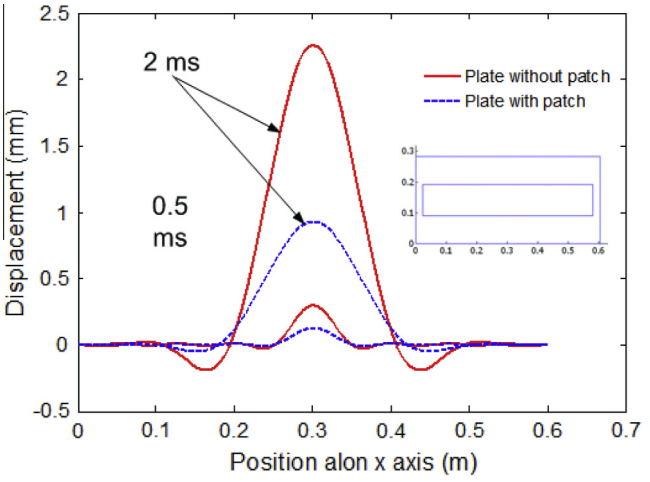

Fig. 14. Comparison between plate with and without PCLD (transverse displacement in section A–A, $h_c = 0.79$ mm, $h_v = 0.127$ mm).

the entire contact from zero to 2 ms, the two curves coincide almost exactly. The shape and amplitude of all crests are nearly identical for the two cases except for a very small difference in amplitude.

For times much greater than contact duration (up to 7.75 ms), the two responses lose concurrence, as shown in Fig. 9. This can be explained by the fact that during the contact time the plate is into forced vibration, so it must submit to the external force. Once the external force is suspended, the boundary conditions begin to influence the evolution of the wave. Indeed, the waves reflected from the edges of the plate do not have the same characteristics since the boundary conditions are different. Clamped edges (CCCC) are stiffer, therefore waves travel faster and reflection appears quicker. Reflected waves cause oscillations subsequent to the initial deformation of the plate.

The two curves begin to diverge almost immediately after the end-of-contact time (Fig. 9).The absolute transverse velocity is less in the simply supported plate than in the clamped plate. At time 6.5 ms for example, the displacement at the impact point of the clamped plate has reached negative values, while in the case of the simply supported plate, the displacement is still almost at its maximum value; yet, the displacement was the same for the two plates at time 2 ms. This behavior is expected since the natural frequencies of the CCCC plate (first frequency at 39.9 Hz) are superior to that of the SSSS plate (first frequency at 29.4 Hz). Noting that the clamps are stiffer than simple supports, the free response in the simply supported plate is slower. To support this result, Fig. 10 shows the velocities for both cases with respect to time. The curves coincide during the contact time, but soon after, the module of the transverse velocity for the CCCC plate becomes higher than for the SSSS plate. As mentioned before, the time at which the curves split depends on the dimensions and properties of the plate.

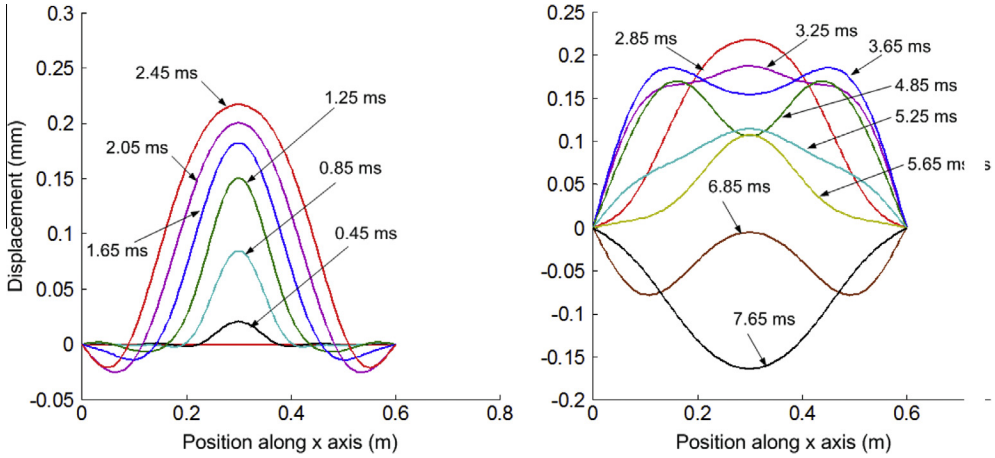

Fig. 16. Transversal displacement in section A–A for thickness ratio $h_v/h_b = 0.1$ (impact at $x = x_b/2$; $y = y_b/2$: during contact (left) and after end-of-contact (right) $h_c = 0.79$ mm, $h_b = 2.38$ mm).

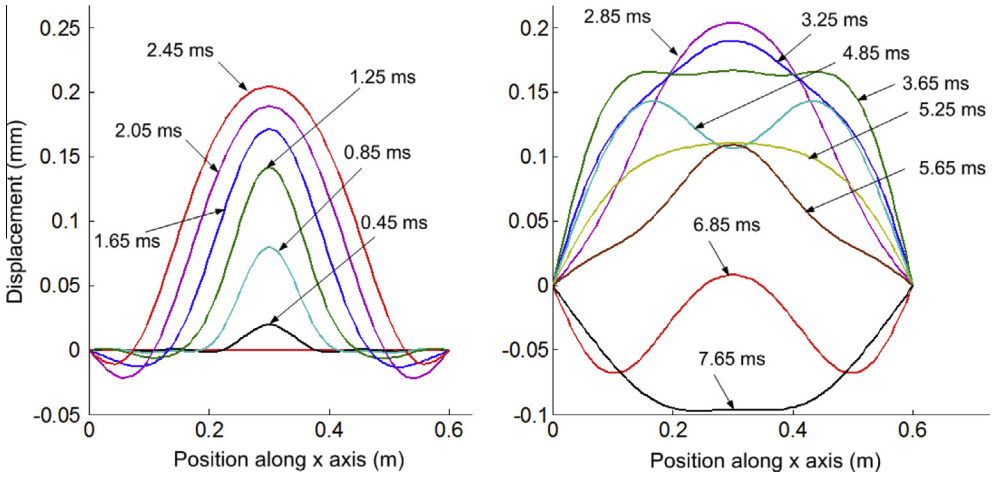

Fig. 17. Transversal displacement in section A–A: ratio $h_v/h_c = 0.1$ (impact at $x = x_b/2$; $y = y_b/2$: during contact (left) and after end-of contact (right) $h_c = 0.79$ mm, $h_b = 2.38$ mm).

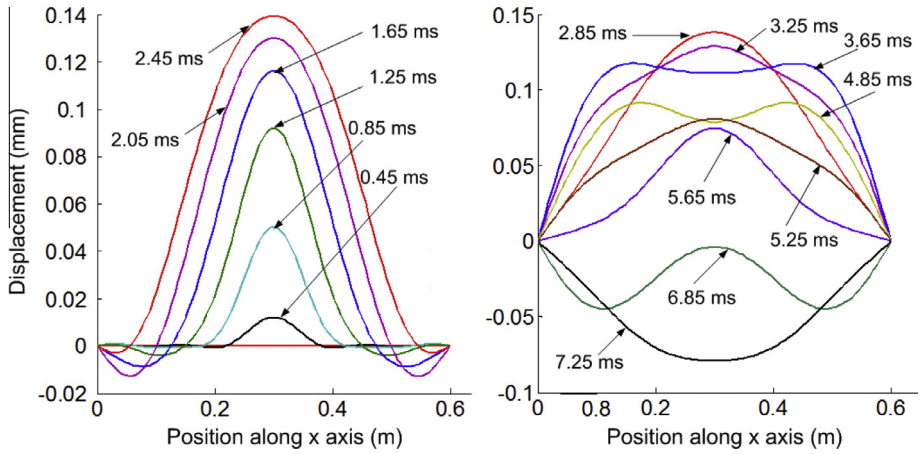

Fig. 18. Transversal displacement in section A–A: ratio $h_c/h_b = 1$ (impact at: $x = x_b/2$; $y = y_b/2$: during contact (left) and after end-of contact (right), $h_v = 0.127$ mm, $h_b = 2.38$ mm).

Fig. 11 shows the evolution of plate deformation in the case of a plate with free boundaries (FFFF). The dynamic behavior differs from the two previous cases (SSSS, CCCC). We see essentially two movements of the plate: relative movement and absolute motion. Relative motion is the same as in the previous two cases: vibration of the plate. The absolute motion is the global displacement of the plate with respect to its original position.

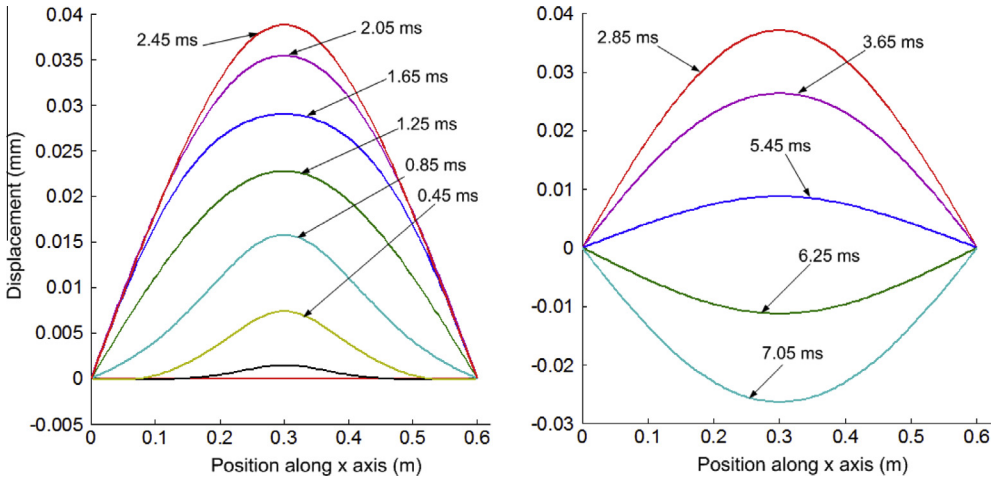

Fig. 19. Transversal displacement in section A–A: ratio $h_c/h_b = 5$ (impact at: $x = x_b/2$; $y = y_b/2$: during contact (left) and after end-of contact (right), $h_v = 0.127$ mm, $h_b = 2.38$ mm).

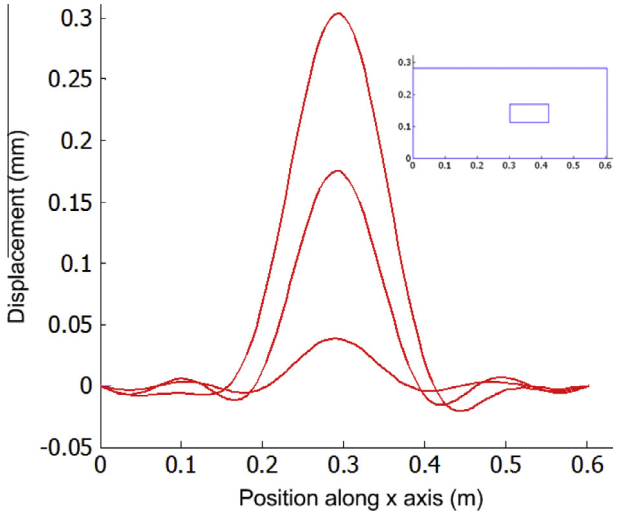

Fig. 20. Transversal displacement in section A–A: influence of PCLD position.

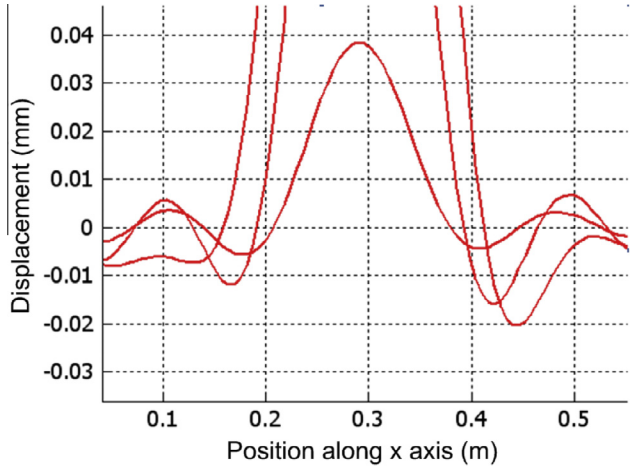

Fig. 21. Zoomed area from Fig. 20.

Furthermore, small wave fronts and low amplitude of main crest are observed compared to SSSS and CCCC. The small size of wave fronts and oscillation of the plate relative to its initial position can be explained by the absence of supports at the borders. The low amplitude of the flexural deformation, compared to the SSSS and CCCC cases, can be explained by the fact that a great part of the impact energy is converted to rigid body displacement while less energy is converted into deformation.

In addition and as said before, the boundary conditions define the characteristics of the reflected wave. In case of FFFF, the crest, which is a result of incident and reflected waves, should have small amplitude, because the reflected wave is weak since the edges are free and they do not have the capacity to reflect the incident wave.

3.1.3. Influence of impact position

Fig. 12 displays the transverse displacement in section A–A with an impact taking place at $x = x_b/5; y = y_b/2$. The figure contains two windows; the left side graph shows the evolution of the wave during the contact time, while the right side graph shows the evolution after the end-of-contact time. It can be seen that during contact time, secondary crests appear to the right side of the main crest as the wave fronts travel in the plate, similar to the behavior with central impact. Fig. 13 displays a 2D representation of the plate deformation at end of contact time. In this figure, it is clear that the wave propagates in all directions. After contact time (right side graph of Fig. 12), as the main crest begins to lose magnitude and to spread out, secondary crests move away from the impact point toward the edge at $x = 0.6$ m. This figure shows that the application of the impact at a point other than plate center leads to a shifting of the main crest due to the wave reflection. This displacement forces the wave fronts to disappear one after the other. When the fronts disappear completely, the main crest begins to recover its amplitude but in the opposite side of its creation, and vice versa up to total disappearance.

The simulations performed on the plate without PCLD show that boundary conditions play an important role in defining the shape, the amplitude, and the evolution of the wave. By including the PCLD in the next section, it will be possible not only to see if the PCLD affects the aforementioned conclusions, but also to identify the influences of the PCLD on the dynamical behavior of the plate.

3.2. Plate with PCLD

In this section, the governing equation is solved in the frequency domain, and the solution is converted back to time domain as explained in the introduction. Again, impacts are simulated at the center of the plate using Eq. (7).

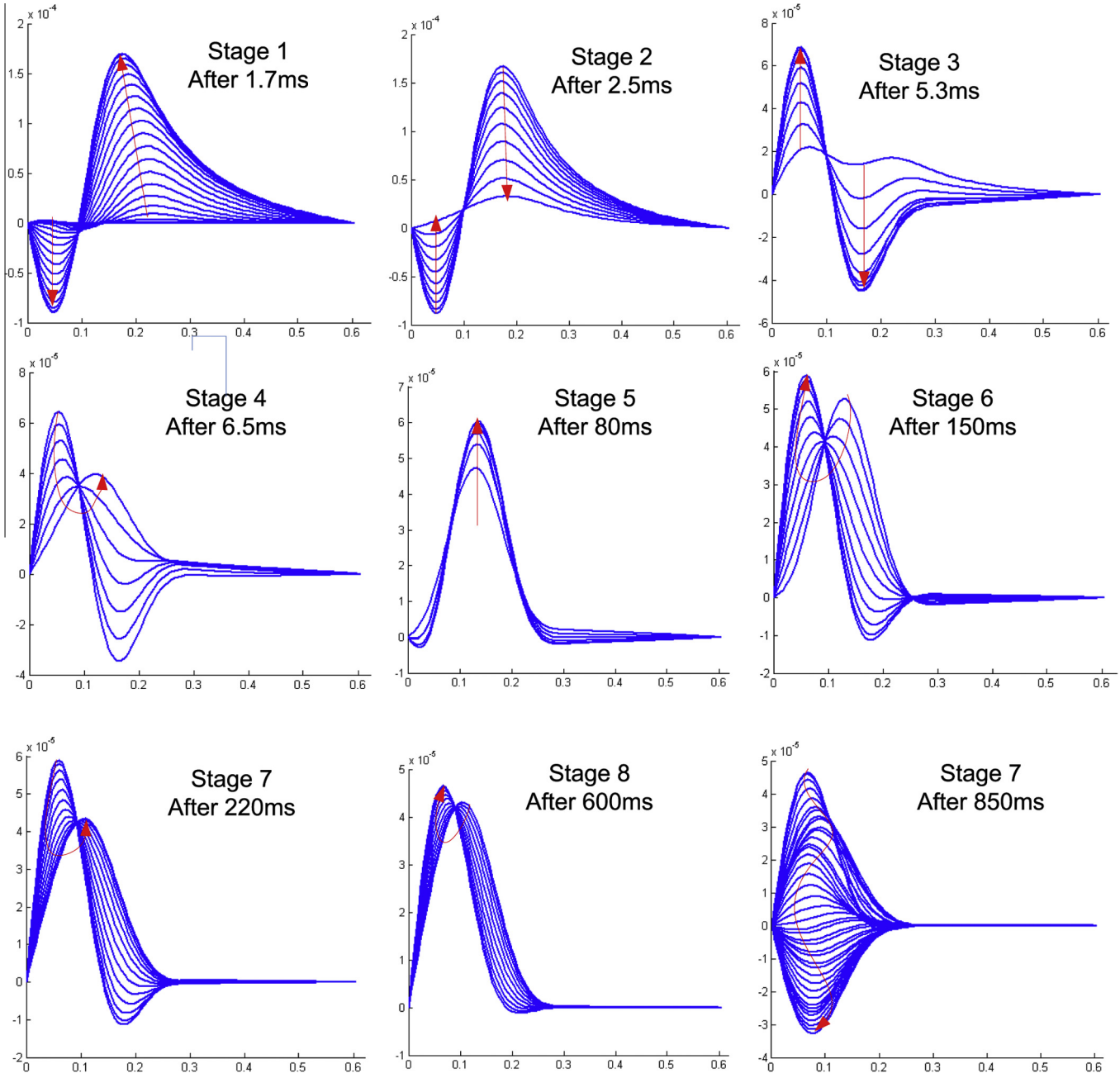

Fig. 22. Transversal displacement in section A–A: influence of CP thickness, (impact at $x = xb/4$; $y = yb/2$).

3.2.1. Influence of PCLD

The PCLD is included to the same plate as the previous section. For all cases studied in the following, simple support (SSSS) boundary conditions are maintained for the plate, while the PCLD has free boundary conditions at all edges. According to Fig. 1, and in all the remainder of the paper unless otherwise indicated; the sandwich has the dimensions mentioned in Table 4:

Figs. 14 and 15 display respectively displacement in sections A-A and B-B. The curves with dashed lines are for plate with PCLD, while curves with solid lines are for plate without PCLD. Two times are represented, 0.5 ms and 2.0 ms. In Fig. 14 (numerical values are provided in Table 5 for purpose of validation), it can be seen that the PCLD reduces the amplitude of the main crest and its transversal speed by about 50%. Neither the width of the main crest nor the amplitude or width of side crests are influenced by PCLD at 0.5 ms. However, at the end-of-contact time (2.0 ms), the main crest is wider in the case of plate with PCLD; side crests are smaller and located farther from the impact. This is due to the different stiffnesses and masses in the two cases. The stiffer the plate is, the less it deforms, and the greater the mass is, the more energy is required to move it. In section B–B (Fig. 15), the locations of PCLD borders are marked with vertical solid lines in order to highlight the influence of discontinuities at the borders. It can be seen that the curvature of the wave at the discontinuity is more important with PCLD, and that the curve in the center of the PCLD area is much flatter. As said before, this is mainly due to the additional stiffness in the area covered by the PCLD.

3.2.2. Influence of PCLD thickness

In this section, we study the influence of the thickness of each layer on the wave propagation in the plate. To analyze the relationship between the proportion of each layer pairs and the behavior of

Table 3
Numerical results plotted in Fig. 6(c) (for purpose of validation).

Position along x axis (m)	Displacement (mm)				
	t = 0.25 ms	t = 0.50 ms	t = 0.65 ms	t = 0.80 ms	t = 1.00 ms
0	0	0	0	0	0
0.054002	−4.41E−05	−6.5167e−005	−3.9264e−005	0.00036751	0.0014189
0.108	7.41E−05	8.7796e−005	0.00037623	0.00072128	−0.00037988
0.16201	−0.00013	0.00015961	0.00013442	−0.0013675	−0.0052115
0.21601	0.000209	−0.00030681	−0.0024533	−0.0049801	−0.0052241
0.27001	−0.0003	−0.0025675	−0.0031743	−0.00020538	0.0084114
0.32401	−0.00025	0.0022977	0.01033	0.021117	0.032833
0.37801	0.002409	0.024357	0.040069	0.049458	0.055545
0.43202	0.017155	0.056364	0.065111	0.066738	0.067072
0.45002	0.019066	0.05962	0.067175	0.067988	0.067853
0.50402	0.006742	0.036027	0.0505	0.057178	0.060867
0.55802	−0.00036	0.0072707	0.019024	0.030721	0.041222
0.61202	−0.00029	−0.0023294	−0.00080466	0.0051236	0.015896
0.66602	0.00015	−0.0010231	−0.0034303	−0.0049634	−0.0023653
0.72003	−0.00012	0.00012438	−0.00047603	−0.002723	−0.0063101
0.77403	0.000117	0.00020024	0.00049172	0.00041774	−0.0018793
0.82803	−0.00012	−0.00013002	4.438e−005	0.00056999	0.0012951
0.88203	0.000102	7.0938e-005	−3.4692e−005	7.9061e−005	0.00064661
0.9000	−7.5661e−018	−7.7302e−018	−6.7525e−019	1.0727e−018	1.0529e−018

Table 4
Values used for patch simulations.

x_b (m)	y_b (m)	h_b (mm)	h_c (mm)	h_v (mm)	x_c (m)	y_c (m)	x_1 (mm)	y_1 (m)
0.601	0.283	0.793	0.793	0.127	0.558	0.1016	25.4	0.0907

Table 5
Numerical results plotted in Fig. 14 (for purpose of validation).

Position along x axis (m)	Displacement (mm)			
	Plate with patch		Plate without patch	
	t = 0.5 ms	t = 0.50 ms	t = 0.5 ms	t = 0.50 ms
0	0	0	0	0
0.054002	−0.00087626	−0.0025855	2.0157e−05	−0.010566
0.108	0.00025714	0.0044553	0.00024004	0.01405
0.16201	−0.00020221	−0.010441	−0.00040386	−0.00023376
0.21601	0.00059702	−0.04874	0.0012002	−0.14112
0.27001	−0.00098427	−1.781e−05	−0.00097717	−0.14247
0.32401	4.0172e−05	0.25735	0.00079696	0.43488
0.37801	0.0043665	0.63879	0.0042266	1.4523
0.43202	0.11312	0.90776	0.26306	2.2025
0.45002	0.1272	0.92875	0.29686	2.2613
0.50402	0.035854	0.75448	0.078348	1.7737
0.55802	−0.0074915	0.3806	−0.019457	0.7527
0.61202	0.0034161	0.061971	0.010263	−0.023484
0.66602	−0.0027809	−0.050782	−0.0067995	−0.18341
0.72003	0.0024089	−0.023218	0.0059584	−0.035584
0.77403	−0.0018658	0.0034342	−0.0050082	0.020401
0.82803	0.0013779	−7.7233e−05	0.0046383	−0.0051308
0.88203	−0.0023816	−0.0024273	−0.0043126	−0.0068747
0.9000	−1.1837e−16	−3.3143e−17	−2.791e−16	−3.2055e−16

the plate, three different thickness ratios are examined: $h_v/h_c, h_v/h_b$ and h_c/h_b. The PCLD configuration is as shown in Fig. 14.

In Fig. 16 and Fig. 17, displacements are taken along section A–A for thickness ratios h_v/h_b of 0.1 and 1.0, respectively. Similar behavior can be observed in the two figures, where only slight variations of the curve shapes occur between the two configurations. However, displacement amplitudes are smaller with higher ratios. Simulations with higher ratios up to 10 showed that the behavior remains the same, with even lower amplitudes. It can be concluded that the VEM has a small effect on the shape of deformation curves, and a greater effect on amplitude. The appearance of wave fronts and the shape of the curve are mainly related to the stiffness of the sandwich. This can be seen in Fig. 18 and 19 where thickness ratio h_c/h_b is studied. The analyses are done for ratios from 0.1 to10. We note that from a value close to 5 the oscillations become purely sinusoidal. This means that the layers of base plate (BP) and constraining plate (CP) allow the sandwich to reach certain stiffness, above which it is not possible for higher modes to occur.

By comparing the case of a plate without PCLD (Section 3.1) and the present cases, it can be concluded that the VEM affect only the

magnitude of displacement, speed and acceleration, on the other hand curve shapes and wave fronts are related to the stiffness of the sandwich.

3.2.3. Influence of PCLD position

In this section, we examine the influence of PCLD position on wave propagation. Fig. 20 displays the transverse displacement in section A–A during contact. In this case, the plate is covered with a PCLD whose characteristics are: $x_1 = 300$ mm,$y_1 = 140$ mm, $x_c = 120$ mm, $y_c = 28$ mm,$h_c = 0.79$ mm, $h_b = 2.38$ mm, $h_v = 0.127$ mm. The PCLD is placed as shown in Fig. 20. We observe that the displacement is not perfectly symmetrical with respect to the impact point: the area where PCLD is applied reacts with a delay due to the inertia that is more important than the other half of the plate (in Fig. 21 a zoom of the wave fronts is shown to highlight this asymmetry). This discrepancy is not only due to VEM damping effect, but also to the added stiffness and mass provided by the constraining layer.

Fig. 22 shows the displacement in section A–A of the plate with on half covered with PCLD ($x_1 = 300$ mm, $y_1 = 0$ mm, $x_c = 300$ mm, $y_c = 281$ mm, $h_c = 7.9$ mm, $h_b = 0.79$ mm, $h_v = 0.127$ mm). The thickness of the CP is ten times that of the BP. In this figure, the evolution of waves due to an impact that took place at the center of the PCLD is represented in nine different stages (periods of time). As seen, the transverse movement of the plate is not sinusoidal. The movement consists of a number of modes that want to appear throughout the plate, but they are quickly attenuated. In fact, attenuation is much greater on the half-plate covered with the PCLD, leaving only the opposite half-plate to vibrate. In the case presented, the covered half of the plate has become so rigid, that the wave cannot spread: the border seems to be moved to the center of the plate.

Finally, it can be concluded that the PCLD postpones the wave and accelerates its damping. This is quite normal since the covered area have a stiffness and surface density much higher than the rest of the plate.

3.3. Conclusion

In this paper, an analytical model to study the propagation of bending waves in rectangular plate with PCLD was described. The equation of motion is obtained by the energy principle and Lagrange equations. The solution is made by two methods. For uncovered plate, the governing equation is solved in time domain. For plate with PCLD the governing equation is solved in frequency domain, then converted back to time domain. Several parameters are analyzed to find their influence on the propagation of bending waves in the sandwich including: boundary conditions, layer thicknesses, position of the impact, and position of PCLD. The simulation results show that stiffer edge supports lead to lower amplitude and higher wave propagation speed. During the contact time, boundary conditions and viscoelastic layer thickness do not affect the wave shape; wave velocity is related to the stiffness provided by constraining layer and base plate. Furthermore, the thickness of the viscoelastic layer plays an important role in the damping of the wave. It not only reduces the transverse speed of the waves, but also lowers the speed of the wave along in-plane direction. If the impact is applied in the middle of the plate, the response is symmetrical. However, if applied elsewhere, the side farthest from the impact will have more wave fronts. If applied very close to an edge, the wave fronts appear on one side of the contact point only. The application of a small, off-center PCLD can cause the response to be asymmetric. It also helps to lower the transverse and longitudinal speeds of the wave in the area on which it is bonded.

Appendix A. Assumed mode functions

The displacements are expressed by:

$$\begin{aligned} u_b(x,y,t) &= \sum_{i=1}^{n_b}\Gamma_i(x,y)U_{bi}(t) = \Gamma^T U_b \\ v_b(x,y,t) &= \sum_{i=1}^{n_b}\Psi_i(x,y)V_{bi}(t) = \Psi^T V_b \\ u_c(x,y,t) &= \sum_{i=1}^{n_c}\Omega_i(x,y)U_{ci}(t) = \Omega^T U_c \\ v_c(x,y,t) &= \sum_{i=1}^{n_c}\Pi_i(x,y)V_{ci}(t) = \Pi^T V_c \\ w(x,y,t) &= \sum_{i=1}^{n_w}\Phi_i(x,y)W_i(t) = \Phi^T W \end{aligned} \tag{A.1}$$

The admissible functions used for the different boundary condition are:

(a) Simply supported all edges (Amabili, 2008)

$$\begin{aligned} \Gamma(x,y) &= \cos\left(\frac{m\pi x}{x_b}\right)\sin\left(\frac{n\pi y}{y_b}\right), \\ \Psi(x,y) &= \sin\left(\frac{m\pi x}{x_b}\right)\cos\left(\frac{n\pi y}{y_b}\right), \\ \Omega(x,y) &= \cos\left(\frac{m\pi x}{x_c}\right)\cos\left(\frac{n\pi y}{y_c}\right), \\ \Pi(x,y) &= \cos\left(\frac{m\pi x}{x_c}\right)\cos\left(\frac{n\pi y}{y_c}\right) \\ \Phi(x,y) &= \sin\left(\frac{m\pi x}{x_b}\right)\sin\left(\frac{n\pi y}{y_b}\right) \end{aligned} \tag{A.2}$$

(b) Clamped all edges (Lall et al., 1987)

$$\begin{aligned} \Gamma(x,y) &= \sin\left(\frac{n\pi y}{x_b}\right)\sin\left(\frac{n\pi y}{y_b}\right), \\ \Psi(x,y) &= \sin\left(\frac{n\pi y}{x_b}\right)\sin\left(\frac{n\pi y}{y_b}\right), \\ \Omega(x,y) &= \cos\left(\frac{m\pi x}{x_c}\right)\cos\left(\frac{n\pi y}{y_c}\right), \\ \Pi(x,y) &= \cos\left(\frac{m\pi x}{x_c}\right)\cos\left(\frac{n\pi y}{y_c}\right) \\ \Phi(x,y) &= \Upsilon(x)\Upsilon(y) \end{aligned} \tag{A.3}$$

$$\begin{aligned} &\Upsilon(x) = A\sin\left(\frac{\gamma x}{L}\right) + B\cos\left(\frac{\gamma x}{L}\right) + C\sinh\left(\frac{\gamma x}{L}\right) + D\cosh\left(\frac{\gamma x}{L}\right), \\ &L = x_b, y_b \end{aligned} \tag{A.4}$$

$A = -1;\ B = \frac{\sin(\gamma)-\sinh(\gamma)}{\cos(\gamma)-\cosh(\gamma)};\ C = 1;\ D = -B$. where γ_i are the solution of the characteristic equation $1 + \cos(\gamma)\cosh(\gamma) = 0$.

(c) Free all edges (Lall et al., 1987)

$$\begin{aligned} \Gamma(x,y) &= \cos\left(\tfrac{m\pi x}{x_b}\right)\cos\left(\tfrac{m\pi x}{y_b}\right), \\ \Psi(x,y) &= \cos\left(\tfrac{m\pi x}{x_b}\right)\cos\left(\tfrac{m\pi x}{y_b}\right), \\ \Omega(x,y) &= \cos\left(\tfrac{m\pi x}{x_c}\right)\cos\left(\tfrac{n\pi y}{y_c}\right), \\ \Pi(x,y) &= \cos\left(\tfrac{m\pi x}{x_c}\right)\cos\left(\tfrac{n\pi y}{y_c}\right) \\ \Phi(x,y) &= \Upsilon(x)\Upsilon(y) \end{aligned} \tag{A.5}$$

$$\Upsilon(x) = A\sin\left(\frac{\gamma x}{L}\right) + B\cos\left(\frac{\gamma x}{L}\right) + C\sinh\left(\frac{\gamma x}{L}\right) + D\cosh\left(\frac{\gamma x}{L}\right) \tag{A.6}$$

where $L = x_b, y_b$; $A = 1; B = \frac{\sin(\gamma)-\sinh(\gamma)}{\cosh(\gamma)-\cos(\gamma)}$; $C = 1$; $D = B$. where γ_i are the solutions of the characteristic equation $1 + \cos(\gamma)\cosh(\gamma) = 0$

References

Baz, A., Ro, J., 1995. Optimum design and control of active constrained layer damping. Journal of Mechanical Design 117, 135.

Baz, A., Ro, J., 1996. Vibration control of plates with active constrained layer damping. Smart Materials and Structures 5, 270.

Baz, A., Ro, J., 1999. Control of sound radiation from a plate into acoustic cavity using ACLD. Smart Materials and Structures 8, 292.

Akbarov, S., Agasiyev, E., Zamanov, A., 2011. Wave propagation in a pre-strained compressible elastic sandwich plate. European Journal of Mechanics-A/Solids 30, 409–422.

Amabili, M., 2008. Nonlinear Vibrations and Stability of Shells and Plates. Cambridge University Press, USA.

Barkanov, E., Rikards, R., Holste, C., Täger, O., 2000. Transient response of sandwich viscoelastic beams, plates, and shells under impulse loading. Mechanics of Composite Materials 36, 215–222.

Baz, A., 1997. Boundary control of beams using active constrained layer damping. Journal of Vibration and Acoustics 119, 166–172.

Baz, A., 1998. Optimization of energy dissipation characteristics of active constrained layer damping, Smart Materials, Structures and MEMS. In: International Society for Optics and Photonics, pp. 668–683.

Blais, J., 2009. Application de l'holographie acoustique en champ proche a l'etude du rayonnement transitoire de plaques soumises a des impacts. Application of near-field acoustic holography to the study of transient radiation plates subjected to impact. Ecole Polytechnique, Montreal (Canada), Canada, p. 231.

Cho, K.D., Han, J.H., Lee, I., 2000. Vibration and damping analysis of laminated plates with fully and partially covered damping layers. Journal of Reinforced Plastics and Composites 19, 1176–1200.

Deu, J.F., Galucio, A.C., Ohayon, R., 2008. Dynamic responses of flexible-link mechanisms with passive/active damping treatment. Computers and Structures 86, 258–265.

Edward, M., Kerwin, J., 1959. Damping of flexural waves by a constrained viscoelastic layer. The Journal of the Acoustical Society of America 31, 952.

Granger, D., Ross, A., 2009. Effects of partial constrained viscoelastic layer damping parameters on the initial transient response of impacted cantilever beams: experimental and numerical results. Journal of Sound and Vibration 321, 45–64.

Haikuo, P., Lin, Y., Guang, M., Kai, S., Fucai, L., 2011. Characteristics of elastic wave propagation in thick beams – when guided waves prevail? Journal of Theoretical and Applied Mechanics 49, 807–823.

Horodinca, M., 2013. A study on actuation power flow produced in an active damping system. Mechanical Systems and Signal Processing 39, 297–315.

Khalfi, B., Ross, A., 2013. Transient response of a plate with partial constrained viscoelastic layer damping. International Journal of Mechanical Sciences 68, 304–312 <http://dx.doi.org/10.1016/j.ijmecsci.2013.01.032>.

Kudela, P., Żak, A., Krawczuk, M., Ostachowicz, W., 2007. Modelling of wave propagation in composite plates using the time domain spectral element method. Journal of Sound and Vibration 302, 728–745.

Lall, A.K., Asnani, N.T., Nakra, B.C., 1987. Vibration and damping analysis of rectangular plate with partially covered constrained viscoelastic layer. Journal of Vibration, Acoustics, Stress, and Reliability in Design 109, 241–247.

Liu, L., Bhattacharya, K., 2009. Wave propagation in a sandwich structure. International Journal of Solids and Structures 46, 3290–3300.

Oulmane, A., 2007. Dynamique transitoire d'une plaque impactee, partiellement recouverte d'un traitement amortissant contraint, (Transient dynamic of impacted plate with partial constraining layer damping). Ecole Polytechnique, Montreal (Canada), Canada, p. 112.

Ray, M., Oh, J., Baz, A., 2001. Active constrained layer damping of thin cylindrical shells. Journal of Sound and Vibration 240, 921–935.

Roy, J.-F., 2005. Etude de la propagation des ondes de flexion dans une plaque amortie subissant un impact, (study of bending wave propagation in a damped plate under the effect of an impact). Universite de Moncton (Canada), Canada, p. 180.

Shorter, P.J., 2004. Wave propagation and damping in linear viscoelastic laminates. The Journal of the Acoustical Society of America 115, 1917–1925.

Sun, D., Luo, S.-N., 2011. Wave propagation and transient response of a FGM plate under a point impact load based on higher-order shear deformation theory. Composite Structures 93, 1474–1484.